This article has been accepted for publication in IEEE Transactions on Transportation Electrification. This is the author's version which has not been fully edited and content may change prior to final publication. Citation information: DOI 10.1109/TTE.2023.3284423

Online Joint Ride-Sharing and Dynamic Vehicle-to-Grid Coordination for Connected Electric Vehicle System

Shiyao Zhang, *Member, IEEE*, and James J.Q. Yu, *Senior Member, IEEE*.

***Abstract*—Connected Electric vehicles (CEVs), as promising core factors in smart cities, take a substantial role in advancing the quality of core transportation services in Intelligent Transportation Systems (ITSs). The application of CEVs triggers the transportability and sustainability of smart cities, especially for ride-sharing and dynamic scheduling operations. Additionally, the combined optimization of the application of these schemes can further contribute to the potential benefits in smart cities. In this paper, an online CEV system for joint ride-sharing and dynamic V2G scheduling is proposed. Specifically, the joint problem is formulated as a mixed-integer quadratic programming (MIQP) problem. To deal with the forecast uncertainties, an online scheduling problem is thereby formulated, which also accounts for the communication effect to the real-time interactions. In the meantime, a bi-level system algorithm is devised to coordinate the CEV operations through the Benders decomposition. The case studies demonstrate that the proposed model can effectively provide high quality citywise ride-sharing and V2G regulation services through reliable vehicular communications. In addition, the computational time of the proposed online bi-level algorithm can be greatly reduced under different network scales. Furthermore, the sufficient utilization of coordinated CEVs can significantly decrease the system operation cost by approximately 43.71% while alleviating city grid stability issues.**

***Index Terms*—Connected electric vehicles, dynamic wireless charging, online framework, ride-sharing, vehicle-to-grid.**

I. Introduction

EMPOWERED by recent data sensing, communication, and processing methods in traffic networks, Intelligent Transportation Systems (ITS), as one of the crucial components in smart cities, are capable of providing various reliable and efficient core transportation services. The aim of ITS is to improve reliable and efficient transportation operations. Compared to conventional ITS, they require the core elements of several emerging technologies by means of connected vehicles (CVs) [1]. Considering the utilization of vehicle-to-everything (V2X), CVs can trigger their installed smart sensors to enable the real-time exchange of self-sensed data information [2], so as to improve the awareness of the surrounding environment of each individual vehicle. Besides, by interacting with the centralized ITS control center under ultra-reliable and low-latency communications, the timely sensing and control for applications of CVs can be guaranteed, e.g. autonomous driving operations [3]. The main purpose is to let the operator to leverage the sensed information for CV driving instructions, while completing the desired ITS objectives, e.g., [4]. For instance, the utilization of CVs in ITS is expected to help reduce traffic congestion through managing a safer and efficient vehicle movement. In the meantime, the related public services can also be facilitated, such as ride-sharing and dynamic wireless charging.

In ITS, ride-sharing is capable of providing passengers with efficient, convenient, and on-demand transportation [5], [6]. Specifically, the ride-sharing scheme is defined as the provision of one vehicle ride service in traffic networks for multiple passengers who have overlapping travel plans. In general, this service is offered through smartphone applications, e.g. Lyft and Uber ride-hailing platforms [7]. Considering the deployment of shared CVs in ITS, ride-sharing operation leads to considerable energy savings and social interactions [8]. Considering the limited vehicles being ultimately deployed in traffic networks while maximizing their occupancy, there are several existing studies [9]–[14] focusing on path-planning strategies while providing ride-sharing services. These approaches achieve promising solutions in the effectiveness of ride-sharing schemes. In [9], [10], autonomous ride-pooling systems were proposed to meet the passengers' demand, and these approaches can also alleviate traffic congestion on the city major roads effectively. Moreover, in [11], by applying a deep reinforcement learning method, the best route was determined based on the sampled historical service requests. Then, a genetic algorithm was devised in [12] for tackling admission control by means of bi-level optimization framework. Besides, in [13], a public vehicle system was built to provide real-time ride-sharing services. This work devised a greedy algorithm to solve the problem that covers the limited number of AVs and system operational costs. Furthermore, an AV dispatching system was proposed in [14] for accounting dynamic taxi trips and capacity adjustment. The aforementioned studies succeed to indicate the benefit of providing ride-sharing services in the modern ITS operation. However, they does not investigate the energy management strategies of the battery-driven CVs when providing ride-sharing services in ITS, e.g. connected electric vehicle (CEV) charging operations.

Manuscript received XX; revised XX; accepted XX (*Corresponding author: James J.Q. Yu*)

This work is supported in part by the Stable Support Plan Program of Shenzhen Natural Science Fund under Grant No. 20220815111111002, and in part by the General Program of Guangdong Basic and Applied Basic Research Foundation No. 2021KQNCX078.

Shiyao Zhang is with the Research Institute for Trustworthy Autonomous Systems, Southern University of Science and Technology, Shenzhen 518055, China (e-mail: zhangsy@sustech.edu.cn)

James J.Q. Yu is with the Department of Computer Science and Engineering, Southern University of Science and Technology, Shenzhen 518055, China (e-mail: yujq3@sustech.edu.cn)

Since the incorporation of remarkable renewable generations in the city smart grid system, the inevitable random and uncorrelated power fluctuations can be occurred due to the intermittency and uncertainty characteristics of renewable generations. In addition, these issues can further jeopardize the stability of the city power grid. In this case, the batteries of CEVs can be collectively utilized to tackle such the issues. In particular, dynamic wireless charging systems become the promising applications to enable CEVs to perform charging when CEVs are moving over the charging facilities. For instance, power supply units, called power tracks (PTs), are installed beneath the traffic roads for facilitating the process of energy transfer [15] so that CEVs can be coordinated to charge in motion. Additionally, [16], [17] developed a vehicular energy network (VEN) based on the operation of dynamic wireless charging to allow the energy transfer from the sources to destinations through electric vehicles (EVs) along appropriate vehicular routes. With the implementation of such facilities, some existing researches have developed dynamic wireless charging protocols by means of EVs [18]–[20]. In [21], a holistic review for EV charging protocols was assessed. [18] investigated and assessed the feasibility of a dynamic charging system under the conditions of EV slow-moving traffic. In [19], an EV dynamic charging system was built to evaluate the EV economic and smart routing operation. The related system model is implemented the fulfillment of the battery energy requirement of these EVs. Moreover, an electric roadway system with limited EV battery capacities and charging rates was proposed in [20] to consider long-distance EV travels. However, the above researches neglect the interaction between the city smart grid and EVs. In practice, improper EV coordinations can further jeopardize the stability of the city smart grid.

The consideration of battery energy demand shall be included when they are connecting to the city smart grid, e.g. vehicle-to-grid (V2G) technologies that enable EVs to store or release energy at appropriate moments and then allow the power exchange between power grid and EVs [22]. [23] examined that according to [24], wireless charging systems can be activated under reliable vehicular communications so as to complete V2G requirements. In addition, CEVs are able to provide various V2G services under coordinated systems [25], which further stabilize the city smart grid system [26], [27]. In this case, V2G coordination refers to an efficient approach of utilizing CEV batteries to restore electricity back to the power system. EVs can be regarded as distributed energy storages that follow the power control signals from the energy market to provide a variety of auxiliary services, e.g. frequency regulation service [26]. Afterwards, the grid fluctuations can be alleviated by the provisioning of V2G regulation services, thereby keeping the grid frequency at its nominal value. [28] developed a hierarchical model to consider the provisioning of joint voltage and frequency regulation services by using EVs. This framework is operated only for EV stationary charging. Considering dynamic EV wireless charging schemes, [29] proposed a dynamic wireless charging system for EVs to consider both the optimal placement of PTs and V2G scheduling with ancillary services. However, these studies solely involve EV charging mechanisms with related tackling strategies to cope with the issues of grid fluctuations. In practice, CEVs can be applied for operating in a multi-service mode in ITS, which includes the provision of at least two or more different public services. In this way, an effective system with multiple types of CEVs is considered.

CEV multi-service mode accounts the interactions among various public services, which can effectively respond to many different demands rather than the conventional way that provides a unilateral service in ITS [30]. By utilizing CEVs, the proposed system framework leverages the interactions and dependencies between the ITS and the city smart grid through efficient information sharing. Several existing studies focus on designing the system models of EVs to provide multiple public services, i.e. [31]–[35]. [31] proposed a joint re-balancing and V2G coordination strategy for the autonomous vehicle (AV) public transportation system. In addition, a novel framework was proposed in [32] for EV optimal parking allocation and charging scheduling, which also considered the provision of the V2G frequency regulation service. In [33], by developing an autonomous vehicle logistic system, AVs can be operated in a joint eco-routing and eco-charging way, as well as providing logistic services. Furthermore, [35] proposed a framework to leverage decentralized deep reinforcement learning and centralized decision making through linear assignment of ride-hailing services for EVs. However, these approaches did not consider the effect of the city wireless communication network. Specifically, the performance of CEV multi-service operations in smart cities can be affected in a substantial manner, since the Internet service has a number of desirable properties, such as decentralization, security, transparency, immutability, and automation [36]. In practice, one of these properties can indeed affect the performance of CEV multi-service operations in ITS, such as unsafe and inefficient lane-changing operations under imperfect communication [37]. By accounting for such effect, a joint routing and charging scheduling optimization problem for the Internet of EVs was formulated in [34] to optimize the system performance. [38] assessed the effect of the communication reliability of a proposed optimal coordinated scheduling framework for EVs. Thus, by implementing the communication factors into the multi-service scheme of CEVs, the reliable and efficient system can be further achieved.

To conclude, the aforementioned works unilaterally provide one single public service for CEVs or execute multi-service operations without the assessment of the communication reliability. To bridge the research gaps, in this work, an online CEV system is developed with the consideration of the joint ride-sharing and dynamic V2G scheduling approach. In particular, the determination of the best CEV commitments is focused for the joint services. Meanwhile, the potential communication effect of CEVs is accounted so as to assess the reliability of the entire system. The main efforts are summarized as follows:

1) The proposed online model encapsulates the featured joint operation for both CEV ride-sharing and dynamic wireless charging in smart cities. Compared to the existing studies, the proposed joint system model can provide high quality multiple CEV services with limited number of CEVs.

This article has been accepted for publication in IEEE Transactions on Transportation Electrification. This is the author's version which has not been fully edited and content may change prior to final publication. Citation information: DOI 10.1109/TTE.2023.3284423

2) An online CEV protocol is implemented between CEVs and the system control center for real-time operations, which is more realistic than [31], [33], [34]. This improves the CEV multi-operation system by formulating a generic problem so as to adapt the model to various citywise traffic networks and energy markets.
3) A bi-level system algorithm is devised to scalably solve the formulated problem through the Benders decomposition method, which can help obtain near-optimal solutions. The benefit of using CEVs in achieving the optimal system social welfare with the provisioning of joint ride-sharing and V2G regulation services is evaluated by the proposed online model.

The rest of this paper is organized in the followings. Section II presents and illustrates the proposed system model. Then, Section III introduces a joint ride-sharing and dynamic V2G scheduling problem. To deal with the forecast uncertainties, Section IV thereby formulates an online problem, as well as the devised bi-level solution. In Section V, the proposed system model is evaluated via different case studies. Finally, this work is concluded in Section VI.

II. System Model

The proposed online CEV system incorporates two major components in ITS, namely, transportation network and CEVs, which will be detailed as follows.

A. Transportation Network

The physical distance of the transportation network is basically determined from one specific location to another inside a particular region. Specifically, the network is modeled as a directed graph $G(\mathcal{V}, \mathcal{E})$, in which the set of road segment intersection points is denoted as $\mathcal{V}$ with the connected edges $\mathcal{E}$. In this case, nodes $i \in \mathcal{V}$ and $j \in \mathcal{V}$ are the locations of the intersection points in the traffic network, which follows $(i, j) \in \mathcal{E}$. Besides, PTs, known as the near-field electromagnetic induction-based wireless power transmission (WPT) devices, are embedded beneath every road segment $(i, j) \in \mathcal{E}$. Based on [39], the type of magnetic and electrostatic induction is considered based on the relevant power levels and gap separations. Moreover, the charging limit to 7.7kW is set by referring to the WPT standard in [40].

B. CEVs

The set of participating CEVs is denoted as $\mathcal{N}$. Each CEV n aims to accomplish either the ride-sharing or dynamic charging requests by moving every road segment $(i, j) \in \mathcal{E}$. For ride-sharing services offered by CEVs, the index set of ride-sharing service requests and passengers are denoted as $\mathcal{R}_s$ and $\mathcal{Z}$, respectively. Each service request shall be accomplished within assigned deadline T_n^{ddl}.

C. System Operations

The entire system operation is comprised of two following stages:

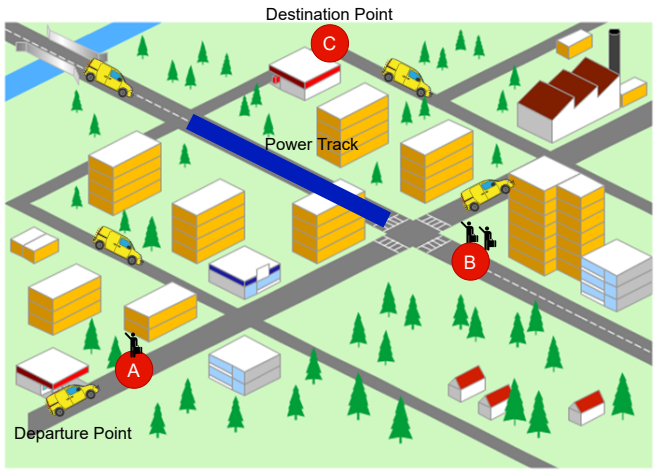

Fig. 1. A simplified example of joint operations.

- **Planning:** The control center initially collects the geometric information of the city road network, the timely ride-sharing requests, and the real-time status of CEVs. Then, it determines the optimal route for CEVs, as well as consider the provision of the joint ride-sharing and dynamic V2G charging service. Specifically, the ride-sharing scheme coordinates the participating CEVs by considering the current vehicle capacity within the total time period, as well as the number of on-demand passengers. Meanwhile, each CEV shall travel more than once to accomplish multiple ride-sharing requests. For dynamic charging scheme, it is incorporated into the execution of the CEV travel plan by providing V2G regulation services, as well as fulfilling the CEV charging requirements. Finally, CEVs are operated to execute the operational plan for implementation.
- **Implementation:** This stage updates the CEV travel plans by accounting for real-time traffic conditions. In the meantime, due to the sudden change of the city traffic network and vehicular status information, the control center of ITS is capable of re-assigning the execution of CEV service plans. The assigning process follows the first-come-first-served basis.

A simplified example of the joint operational schemes is presented in Fig. 1. First of all, CEV n starts from the initial point A and reaches the nearest point to pick up the passenger 1. Then, it travels to point B to pick up the passengers 2 and 3 based on its available capacity. After that, CEV n proceeds to point C to complete the ride-sharing task since the destinations of these three passengers are all point C. Meanwhile, the travel plan from point B to point C needs to consider the charging service. Hence, the traveling trajectory of CEV n may include the road segments embedded with PTs, which is labeled as a blue bold line in Fig. 1. Last but not least, the n-th CEV approaches its final destination, point C, to accomplish the ride-sharing service plan before the deadline. In real-world operation, it is possible that when having a larger on-demand quantity to pick up more passengers for every request.

TABLE I
NOTATIONS FOR THE PROPOSED SYSTEM.

Parameters	
$\mathcal{V}$	Index set of nodes
$\|\mathcal{V}\|$	Total number of nodes
$\mathcal{E}$	Index set of road paths
$\mathcal{E}$	Total number of road paths
$\mathcal{T}$	Index set of timeslot
$\|\mathcal{T}\|$	Total operation time period
Δt	Length of a time slot
$\mathcal{N}$	Index set of CEVs
$\|\mathcal{N}\|$	Total number of CEVs
$\mathcal{Z}$	Index set of passengers
$\mathcal{R}_s$	Index set of ride-sharing requests
$\mathcal{L}_n^{\text{dlv}}$	Set of delivery node of CEV n
L_n^{src}	Departure point (source) of CEV n
L_n^{dst}	Destination point of CEV n
T_j^{wait}	Maximum waiting time for passengers at node j
T_n^{ddl}	Service deadline of CEV n
$T_{ij,n}$	Travel time of CEV n on road (i,j)
$T_{n,r}^{\min}$	Minimum service time for CEV n at request r
$T_{n,r}^{\max}$	Maximum service time for CEV n at request r
$q_{i,n}$	Changing number of passengers of CEV n at node i
$y_{(i,j),t}$	Energy indicator of PTs for road (i,j) at time t
P_n^{dch}	Maximum discharging power of EV n
P_n^{ch}	Maximum charging power limit of EV n
η_{ch}	Charging efficiency
η_{dch}	Discharging efficiency
$d_{ij,n,t}$	Travel distance of CEV n for road (i,j) at time t
$\overline{v}_{ij,n,t}$	Average speed of CEV n for road (i,j) at time t
β_n	Unit energy consumption of CEV n
C_n	Installed battery capacity of CEV n
$S_n^{L_n^{\text{src}}}$	SOC of CEV n at departure point
S_n^{req}	Charging requirements of CEV n
$S_n^{\min}$	Lower limit of SOC for CEV n
$S_n^{\max}$	Upper limit of SOC for CEV n
$I_{n,t}$	Binary variable of whether CEV n is collected at time t
σ_t	Probability of packet loss
F^{RS}	Total ride-sharing cost function
F^{V2G}	Total dynamic V2G coordination cost function
P_t^{tot}	Total system active power at time t
P_t^{reg}	Regulation signals at time t
e_t	Forecast error at time t
α_n	Unit routing cost of CEV n
γ_n	Unit transportation service cost of CEV n
λ_n	Charging/discharging cost for CEV n
R^{base}	Base reward for providing V2G regulation service
ξ	Penalty factor for performance of regulation service
r_t	Ride-sharing service request at time t
D	Size of a one-dimensional control variable
m_s	Number of iteration
F_t^{RS}	Total ride-sharing cost function at time t
F_t^{V2G}	Total dynamic V2G coordination cost function at time t
S_n^{ms}	Margin of safety of CEV n
μ	Size of margin of safety
Ω_t	Representation of Benders cuts at time t
ϵ	Optimality gap
$\overline{F_t^{\text{RS}}}$	Upper bound of ride-sharing operation cost
$F_t^{*\text{RS}}$	Optimal ride-sharing operation cost
M_o	Maximum iteration number of online algorithm
Optimization variables	
$x_{ij,n,t}$	Binary variable of whether CEV n travels road (i,j) at time t
$k_{j,n}$	Staying duration of CEV n at node j
$\tau_{j,n}$	Time of arrival of CEV n at node j
$W_{j,n}$	Capacity of CEV n at node j
$P_{n,t}$	Active power of CEV n at time t
$S_{n,t}$	SOC of CEV n at time t

III. PROBLEM FORMULATION

The system framework of the CEV system is developed based on joint ride-sharing and dynamic V2G scheduling. The problem formulation is presented as follows. The key variables and parameters are presented in Table I.

A. Ride-Sharing Constraints

The proposed ride-sharing scheme encompasses two main operations: CEV routing and ride-sharing. To ensure real-world applications, CEV operations shall be performed satisfying several constraints shown in the sequel.

A binary variable $x_{ij,n,t}$ is first introduced to indicate whether CEV $n \in \mathcal{N}$ traverses the road $(i,j) \in \mathcal{E}$ at time t, and it includes

$$x_{ij,n,t} = \begin{cases} 1 & \text{if CEV } n \text{ traverses the road } (i,j) \text{ at time } t, \\ 0 & \text{otherwise.} \end{cases} \tag{1}$$

Then, $\tau_{j,n} \geq 0$ is introduced as the arrival time of CEV n at node j. This variable also indicates the cumulative time consumption of CEV n, in which it is different from the time index t. After each request being assigned, CEV n shall approach the final destination for the ride-sharing operation. This indicates that it has to traverse at least one portion of the traffic network, which can be ensured by

$$\sum_{t\in\mathcal{T}, i\in\mathcal{V}} x_{ij,n,t} \geq 1, \ \forall n \in \mathcal{N}, j \in \{\mathcal{L}_n^{\text{dlv}}\}, \tag{2}$$

where $\mathcal{L}_n^{\text{dlv}}$ denotes the delivery location set of AV n.

The CEV network flow model is developed based on the road network topology. Suppose $\sum_{t\in\mathcal{T}, i\in\mathcal{V}} x_{ij,n,t}$ and $\sum_{t\in\mathcal{T}, i\in\mathcal{V}} x_{ji,n,t}$ be the incoming and outgoing vehicular flows, respectively. The connectivity of multiple consecutive roads are ensured by

$$\sum_{t\in\mathcal{T}, i\in\mathcal{V}} (x_{ij,n,t} - x_{ji,n,t}) = \begin{cases} 1 & \text{if } j = L_n^{\text{dst}}, L_n^{\text{src}} \neq L_n^{\text{dst}}, \\ -1 & \text{if } j = L_n^{\text{src}}, L_n^{\text{src}} \neq L_n^{\text{dst}}, \\ 0 & \text{otherwise,} \end{cases} \tag{3}$$

where L_n^{src} and L_n^{dst} represent the departure and destination points of the n-th CEV's route. According to (3), the first two conditions guarantee that if CEV n reaches the node j, there shall be incoming and outgoing vehicular flows between the departure and destination points, respectively, which guarantees the connectivity of vehicular routes.

Besides, several road access conditions may be restricted for certain vehicles. For instance, some particular types of vehicles are not allowed to travel over certain road portions. In this work, the implementation of various types of vehicles is considered, e.g. public and private cars. To address such realistic scenarios, the restricted zone with the set of nodes $\mathcal{V}' \subset \mathcal{V}$ and the connected edges $\mathcal{E}' \subset \mathcal{E}$ is first defined. When there is a restriction on road (i,j) for CEV n, $x_{ij,n,t} = 0, \ \forall i \in \mathcal{V}', j \in \mathcal{E}', t \in \mathcal{T}$ is defined to satisfy this condition. This case indicates that CEV n cannot travel between point i and point j due to the region of the restricted zone.

The proposed ride-sharing operation needs to consider the waiting time for passenger pickups for the purpose of measuring the provisioning of these services. When CEV n needs to perform pickup tasks related to certain number of passengers, the waiting time for this vehicle to load or unload passengers at node $j \in \mathcal{V}$ is denoted by

$$k_{j,n} \leq T_j^{\text{wait}}, \ \forall n \in \mathcal{N}, r \in \mathcal{R}_s, \tag{4}$$

where T_j^{wait} denotes the maximum allowable waiting time for passengers at node j.

In addition, $\tau_{j,n}$ is first defined as the arrival time of CEV n at node j and it is updated when it accomplish all ride-sharing service requests $\mathcal{R}_s$. After that, when the CEV $n \in \mathcal{N}$ travels over $(i,j) \in \mathcal{E}\backslash\{\mathcal{E}'\}$, the variable $\tau_{j,n}$ is greater than the required traveling time plus the passengers' picking-up/dropping-off time, which is described as

$$\tau_{j,n} \geq \tau_{i,n} + k_{i,n} + T_{ij,n}, \ \forall x_{ij,n,t} = 1, \tag{5}$$

where $T_{ij,n}$ is the travel time for CEV $n \in \mathcal{N}$. Then, the time for passengers to approach the destination point can be represented by

$$T_{n,r}^{\min} \leq \tau_{j,n} \leq T_{n,r}^{\max}, \ \forall r \in \mathcal{R}_s, \tag{6}$$

where $T_{n,r}^{\min}$ and $T_{n,r}^{\max}$ are the allowable minimum and maximum times at request r, respectively. Then, the deadline for ride-sharing services at point L_n^{dst} for the n-th CEV, T_n^{ddl}, follows

$$\tau_{L_{\text{dst}}^n,n} \leq T_n^{\text{ddl}}, \ \forall n \in \mathcal{N}. \tag{7}$$

Furthermore, the vehicle capacity is modeled by considering the change of the holding number of passengers during ride-sharing services. Suppose $W_{j,n}$ be the loading capacity of CEV n at node j. Then, the residual capacity of CEV $n \in \mathcal{N}$ will be no less than the vehicle capacity at node i, which is described as

$$W_{j,n} \geq W_{i,n} + q_{i,n}, \ \forall x_{ij,n,t} = 1, \tag{8}$$

where $q_{i,n}$ is the number of loading capacity of CEV n for passengers at node i, which is obtained based on the number of service requests. When CEV n accomplish the service request $r \in \mathcal{R}_s$, the variable $W_{j,n}$ is also updated.

B. Dynamic V2G Scheduling Constraints

With the known PT placement information in the city traffic network, the dynamic wireless charging/discharging for the CEVs can be scheduled for their preference to participate. The rest of CEVs are regarded as the vehicle fleet that only traverses in the road network. Hence, by considering the charging/discharging mechanisms, the charging and discharging powers of CEV $n \in \mathcal{N}$ follow

$$P_n^{\text{dch}} \leq y_{(i,j),t} P_{n,t} \leq P_n^{\text{ch}}, \ \forall t \in \mathcal{T}, \tag{9}$$

where $y_{(i,j),t}$ is the energy activation indicator of PTs that are installed over road $(i,j) \in \mathcal{E}$ at time t.

The state-of-charge (SOC) of the participated CEV $n \in \mathcal{N}$ at time $t \in \mathcal{T}$ is further defined and obtained by

$$S_{n,t+\Delta t} = S_{n,t} + \frac{\Delta t}{C_n} \eta(P_{n,t}) P_{n,t}, \tag{10}$$

where C_n is the battery capacity. Moreover, $\eta(\cdot)$ is the efficiency of the charging and discharging powers, which can be obtained by

$$\eta(P_{n,t}) = \begin{cases} \eta^{\text{ch}} & \text{if } P_{n,t} \geq 0, \\ \frac{1}{\eta^{\text{dch}}} & \text{if } P_{n,t} < 0, \end{cases} \tag{11}$$

where $\eta^{\text{ch}}, \eta^{\text{dch}} \in (0,1]$ are the related energy efficiencies for charging and discharging schemes, respectively. In practice, the changes of the air gap distance can indeed incur the lower efficiency and instabilities in the system. Hence, based on [41], ϑ is introduced as the degradation factor for the lower efficiency case due to the changes of the air gap distance in each PT. Then, the efficiency of the charging and discharging powers can be modified as $\widetilde{\eta}(P_{n,t}) = \vartheta \eta(P_{n,t})$, which further affects the performance of dynamic V2G scheduling model.

Since CEVs travel over the traffic network, the related travel distance of CEV n is defined as $d_{ij,n,t}$, which also follows $d_{ij,n,t} = \overline{v}_{ij,n,t} T_{ij,n}$. Then, the real-time battery energy consumption of CEV $n \in \mathcal{N}$ is expressed as

$$S_{n,t+\Delta t} := S_{n,t} - \frac{\beta_n}{C_n} d_{ij,n,t} \tag{12}$$

where β_n is the unit energy consumption factor of CEV n.

Apart from energy consumption when the participated CEV n is traveling, it must fulfill the energy requirement associated with its charging/discharging behaviors. The energy requirement of each CEV n is directly obtained by its required SOC level, which is denoted as S_n^{req}. For each CEV n, suppose S_{n,L_{src}^n} be the initial SOC and S_{n,L_{dst}^n} be the final SOC. Then, during the entire time period, for the participated CEV $n \in \mathcal{N}$, it follows

$$S_n^{L_{\text{dst}}^n} \geq S_n^{L_{\text{src}}^n} + S_n^{\text{req}}. \tag{13}$$

Besides, the dynamic V2G scheduling scheme have to avoid the over-charging and deep-discharging cases. Hence, the scheme follows the operational bounds of SOC of CEV n at time t as

$$S_n^{\min} \leq S_{n,t} \leq S_n^{\max}, \tag{14}$$

where $S_n^{\min}$ and $S_n^{\max}$ denote the minimum and maximum limits in SOC of CEV n, respectively.

C. Communication Constraints

The imperfect communication constraints are derived based on two aspects, including imperfect communications on renewable energy resources (RESs) and imperfect CEV communications. According to [42], imperfect communication can easily lead to a large packet loss probability so as to affect the RESs prediction and V2G dispatch performance. In addition, due to the stochastic and intermittency characteristics of RESs, the actual output of active power signals cannot be accurate. Thus, the imperfect communication of the regulation signals is modeled that includes the information errors as $P_t^{\text{reg}} = (1 + e_t) P_t^{\text{reg}}$ where $e_t \sim N(0, 0.3)$, by following [29].

Besides, communication constraints also include the reliability of the smart meters installed in CEV wireless chargers. Hence, in practice, the imperfect communications are related to real-time SOC and CEV operational time to the control

center. The packet loss during the communication phase may easily occur because of data communication time constraints [43]. Specifically, if the data packets are unavailable, the information of SOC and operational status lacks so that the scheduling performance would be degraded. In such case, the related communication constraint is modeled as

$$I_{n,t} = \begin{cases} 1 & \text{with probability of } \sigma_t, \\ 0 & \text{with probability of } 1-\sigma_t, \end{cases} \tag{15}$$

where $I_{n,t}$ is a binary variable to assess whether CEV n is collected under the packet loss probability of σ_t at time t or not. Then, (15) is implemented over the conditions of (4), (5), (10), and (12) to indicate the possible travel delay and unavailability of SOC level due to packet loss during the meter data communications, whereas it affects the values of $k_{j,n}$, $\tau_{i,n}$, $P_{n,t}$, and $d_{ij,n,t}$ by multiplying $I_{n,t}$.

Furthermore, the control center can broadcast the operation signals centrally to all CEVs after receiving the information of both the energy market and traffic network. Let D be the size of a one-dimensional control variable. Due to the potential for heavy communication between the control center and the participating CEVs, the large quantity of CEV fleets may simultaneously generate the communication burden among the communication nodes. In this case, the communication overhead in the system framework is defined as

$$CO = D \cdot m_s \cdot |\mathcal{T}|(|\mathcal{N}|+1), \tag{16}$$

where m_s denotes the number of iterations taken in the procedure.

D. Formulation of Multi-Objective Problem

The proposed CEV system is developed to account the joint ride-sharing and dynamic V2G scheduling problem. For the ride-sharing scheme, the related operation is associated with the travel distance of the n-th CEV [33]. In addition, it involves the system operational cost for the ride-sharing operations that guarantee the satisfaction of the passengers since the residual service time for each time slot shall be reduced. Therefore, the related ride-sharing cost function can be described by

$$F^{\text{RS}} = \sum_{t\in\mathcal{T}, n\in\mathcal{N}} \left(\sum_{(i,j)\in\mathcal{E}} \alpha_n d_{ij,n,t} x_{ij,n,t} + \gamma_n \tau_{L_n^{\text{dst}},n} \right), \tag{17}$$

where γ_n represents the unit transportation service cost of CEV n and α_n is the unit CEV traveling cost.

Besides, the V2G coordination problem is related to the CEV dynamic wireless charging operation by fulfilling their charging requirements, as well as the provisioning of V2G regulation services. By following [29], the relevant operational cost is directly associated with the management of the CEV fleets within $\mathcal{T}$ on performing dynamic V2G scheduling, which can incur the CEV charging/discharging cost. Moreover, the system stability requirements are kept by means of V2G regulation services that can smooth out the city smart grid's active power fluctuations so as to keep the grid frequency within a stable range. Based on these aspects, the dynamic V2G coordination cost function can be calculated by

$$F^{\text{V2G}} = \sum_{t\in\mathcal{T}} \sum_{n\in\mathcal{N}} \lambda_n I_{n,t} P_{n,t} - R_{\mathcal{N}}, \tag{18}$$

where λ_n is the unit charging cost for CEV n and it varies with the change of time t. $R_{\mathcal{N}}$ represents the reward for the provisioning of regulation services, which follows:

$$R_{\mathcal{N}} = \left(R^{\text{base}} - \xi \sum_{t\in\mathcal{T}} |P_t^{\text{tot}}| \right), \tag{19}$$

where $\xi \in (0,1]$ is the penalty parameter to investigate the regulation performance, and R^{base} is the base reward. In addition, the regulation reward is divided based on their battery capacities among the participated CEVs. In particular, it can be divided by the certain ratio of $|\mathcal{N}|$, in which the ratio is related to the battery capacity of CEV n and the entire battery capacities of all CEVs. This is to ensure the fair regulation reward allocation for each CEV. $P^{\text{tot}}(\mathcal{T})$ is further denoted as the grid power profile. This can be calculated by

$$P_{\mathcal{T}}^{\text{tot}} = P_{\mathcal{T}}^{\text{reg}} + \sum_{n\in\mathcal{N}} P_{n,\mathcal{T}}, \tag{20}$$

where $P^{\text{reg}}(\mathcal{T})$ is the regulation signals and $P_n(\mathcal{T})$ is the CEV n power profile. By focusing (19), the proposed V2G coordination is developed to gaining the reward for the provisioning of the V2G regulation service, while minimizing the related charging costs. Thus, the proposed joint problem is formulated as

$$\textbf{minimize} \quad F^{\text{RS}} + F^{\text{V2G}}, \tag{21a}$$

$$\textbf{subject to} \quad (2)-(10), (12)-(14). \tag{21b}$$

E. Linear Transformation

In (21), the constraints (5) and (8) cannot be modeled directly without prior information on $x_{ij,n,t}$, since the condition $x_{ij,n,t} = 1$ should hold. Hence, (5) and (8) are attempted to be converted into the equivalent linear forms. Prior to that, the following two cases are taken into account:

- Case 1: If $x_{ij,n,t} = 0$, starting from point i through $(i,j) \in \mathcal{E}$, CEV n won't visit point j. Since $\tau_{j,n}$ is constrained within a feasible region, there is no relationship between $\tau_{i,n}$ and $\tau_{j,n}$. Similar to this, $W_{i,n}$ and $W_{j,n}$ have no direct relation.
- Case 2: If $x_{ij,n,t} = 1$, $\tau_{j,n}$ must be greater or equal to the right hand side of constraint (5).

Then, constraints (5) and (8) are transformed into the equivalent linear forms by using the big-M reformulation as

$$\tau_{j,n} \geq \tau_{i,n} + k_{i,n} + T_{ij,n} - M(1 - x_{ij,n,t}), \tag{22}$$

$$W_{j,n} \geq W_{i,n} + q_{i,n} - M(1 - x_{ij,n,t}). \tag{23}$$

By having the above linear transformation, the proposed joint problem is presented as

$$\textbf{minimize } F^{\text{RS}} + F^{\text{V2G}}, \tag{24a}$$

$$\textbf{subject to } (2)-(4), (6), (7), (9), (10), (12)-(14), (21), (23). \tag{24b}$$

IV. Online CEV Framework

This section develops the system framework of online CEV system considering joint ride-sharing and dynamic V2G scheduling. The problem formulation and the devised online bi-level algorithm are presented in the following.

A. Formulation of Online Joint Problem

In real-world operations, the ride-sharing and city power demands of smart cities are tackled in a real-time manner. Therefore, it is even realistic to propose an online joint problem for CEVs. At each time slot, the smart system receives the real-time ride-sharing requests r_t and regulation signal P_t^{reg}, and then coordinates the participated CEVs to provide the joint services immediately. Hence, considering the real-time ride-sharing operation, (18) can be presented as:

$$F_t^{\text{RS}} = \sum_{n\in\mathcal{N}} \left(\sum_{(i,j)\in\mathcal{E}} \alpha_n d_{ij,n,t} x_{ij,n,t} + \gamma_n (\tau_{L_n^{\text{dst}},n} - t) \right). \quad (25)$$

For dynamic V2G scheduling, (18) is transformed as following function for online V2G scheduling:

$$F_t^{\text{V2G}} = \sum_{n\in\mathcal{N}} \lambda_n P_{n,t} - \left(\frac{R^{\text{base}}}{|\mathcal{T}|} - \xi |P_t^{\text{tot}} - P_{t-1}^{\text{tot}}| \right), \quad (26)$$

Based on constraints (10), (13), and (14), for online V2G scheduling, CEV n shall fulfill the charging requirement as

$$\begin{aligned} S_{n,t} + \eta(P_{n,t}) P_{n,t} \Delta t + \eta^{\text{ch}} P_n^{\text{ch}} (|\mathcal{T}| - t - 1)\Delta t \\ \geq S_n^{\text{req}} + S_{n,t}^{\text{ms}},\ \forall t \leq |\mathcal{T}| - 1. \end{aligned} \quad (27)$$

In this constraint, the left-hand side of the inequality above shows the maximum SOC to be charged for CEV n and the vehicle power profile $P_{n,t}$, while the safety margin, denoted as $\mu \in [0, 1]$, is utilized to deal with the real-time information uncertainty and it is shown on the right-hand side. The aim is to increase the energy buffer in CEV n to accommodate with the uncertainty. Then, it holds

$$S_{n,t}^{\text{ms}} = \mu (S_n^{\max} - S_n^{\text{req}}). \quad (28)$$

Furthermore, it is anticipated that the lifespan of CEV batteries will be affected by their fast and frequent charging/discharging behaviors while using their V2G capabilities to provide frequency regulation services. In this case, a penalty term is introduced to the objective function in (26) to cope with the battery degradation issue. This term aims to penalize the fast charging/discharging behaviors of CEV batteries, and then the modified objective function is updated as $\widetilde{F}_t^{\text{V2G}} = F_t^{\text{V2G}} + \sum_{n\in\mathcal{N}} (P_{n,t})^2$.

To sum up, the online joint optimization problem can be expressed as:

$$\textbf{minimize}\ F_t^{\text{RS}} + F_t^{\text{V2G}}, \quad (29a)$$

$$\textbf{subject to}\ (24b)\ \text{and}\ (27). \quad (29b)$$

B. Decomposition

The ride-sharing and dynamic scheduling constraints are included in the proposed online joint model. The operational constraints are mostly related to the CEV mechanism. As the number of CEVs increases, the constraints appear to be more complex since the joint operation is accounted. Since the formulated problem is solved real-time, the system still explodes with the number of CEVs increasing due to the complicated CEV constraints. Hence, to solve the problem in an efficient manner, the Benders decomposition is utilized to resolve the mixed integer linear programming (MILP) problem, in which [44] implies that this method is suitable.

By taking $x_{ij,n,t}$ as a connecting variable, the original problem can be transformed as a bi-level problem. The master problem (MP) aims to minimize the system cost that is incurred by the ride-sharing operation with the related constraints, which is the MILP problem shown as

$$\textbf{minimize}\ F_t^{\text{RS}} + \Omega_t, \quad (30a)$$

$$\textbf{subject to}\ \Omega_t \geq 0, \quad (30b)$$

$$(2) - (4), (6), (7), (21), (23), \quad (30c)$$

where Ω_t is the representation of Benders cuts for the MP. The Bender cuts are added as penalty term and a extra constraint to the MP, in which it satisfies

$$\Omega_t \geq 0,\ \forall t \in \mathcal{T}. \quad (31)$$

In this case, the Benders cuts are implemented to the MP as the additional constraint so as to adjust the system schedule on ride-sharing and CEV dynamic scheduling operations. Even though each CEV charging/discharging constraints are not involved by MP directly, they are embedded as the Benders cuts in an implicit manner. With the increasing number of iterations, the number of cuts raises and the entire model are regarded by the control center via the generated cuts. In the meantime, the consideration of the CEV dynamic scheduling constraints in MP can become increasing accurate and complete such that the violation can be reduced gradually with the iteration proceeding.

Since the dynamic scheduling constraints are not considered, the reformed MP is simplified. Then, it is ensured that the operational cost $F_t^{,\text{RS}}$ gained by solving the MP should not be larger than the solution obtained in the primal model that denotes as $F_t^{*\text{RS}}$, which shows

$$F_t^{,\text{RS}} \leq F_t^{*\text{RS}}. \quad (32)$$

Since the CEV dynamic V2G scheduling scheme is not involved, the final solution $x_{ij,n,t}^{,}$ obtained by solving the MP may not be feasible. Hence, the related adjustment of using the Benders cuts is crucial for checking the feasibility of the sub-problem (SP) formulated at the lower level. The SP is formulated as follows:

$$\textbf{minimize}\ F_t^{\text{V2G}}, \quad (33a)$$

$$\textbf{subject to}\ x_{ij,n,t} == x_{ij,n,t}^{,}, \quad (33b)$$

$$(9), (10), (12) - (14). \quad (33c)$$

For the SP shown in (33), the optimal solutions obtained by the MP are utilized so as to check the feasibility of the solution. The gap index to evaluate the optimality of the feasible scheme is defined as

$$\epsilon = \frac{\overline{F_t^{\text{RS}}} - F_t^{,\text{RS}}}{F_t^{,\text{RS}}}, \quad (34)$$

where $\overline{F_t^{\text{RS}}}$ is the upper bound of the operation cost and it satisfies $F_t^{*\text{RS}} \leq \overline{F_t^{\text{RS}}}$.

Thus, more cuts are added to the constraints of the MP so that the value of $F_t^{'\text{RS}}$ would not decrease. Besides, if the best

feasible solution is obtained, $\overline{F_t^{\text{RS}}}$ would not increase. Hence, it is apparent that the gap index function (34) is a decreasing function that is related to the iteration number. When the gap index is small, the stopping criterion is reached for the chosen $\overline{F_t^{\text{RS}}}$ as the final result.

C. Bi-Level System Algorithm

Algorithm 1 presents the devised online bi-level algorithm, which is performed at each time slot. Initially, the system receives the information of road network, total operational period, and number of participating CEVs. Then, at each time t, the system obtains the ride-sharing request r_t and regulation signal P_t^{reg}. For each iteration m, the system solves the MP by obtaining the optimal solution $x_{ij,n,t}(m)$, $\tau_{j,n}(m)$, and $W_{j,n}(m)$ that are related to the solution set $x^{:}_{ij,n,t}$, $\tau^{:}_{j,n}$, and $W^{:}_{j,n}$ shown in the previous subsection. By taking these results into the SP, the system solves the SP to obtain each CEV's charging/discharging decision $P_{n,t}(m)$. In this case, the feasible solution is obtained by solving the SP at the lower level, and then this result is substituted into the MP at the upper level. The ride-sharing scheme is scheduled and the upper bound of the system cost is obtained correspondingly. In every round of the iteration, the optimal decisions are adjusted based on the control signal at time t. Then, each CEV can report its new decision to the system. Furthermore, to reach the stopping criterion, the condition $m = M_o$ is defined to ensure the approach of the maximum iteration number.

Algorithm 1 Proposed online bi-level algorithm

1: Given road network, total time period $\mathcal{T}$, and $|\mathcal{N}|$ participating CEVs participated.
2: **for** t = 1: $|\mathcal{T}|$ **do**
3: Given ride-sharing request $r_t \in \mathcal{R}_s$ and regulation signal P_t^{reg}.
4: **for** n = 1: $|\mathcal{N}|$ **do**
5: **for** m = 1: M_o **do**
6: Solve (30) to obtain $x_{ij,n,t}(m)$, $\tau_{j,n}(m)$, and $W_{j,n}(m)$ at the upper level.
7: Solve (33) to obtain $P_{n,t}(m)$ at the lower level.
8: Obtain the feasible solution in step 7, and substitute it into (30).
9: **if** the stopping criterion met by checking ϵ **then**
10: Update the optimal solutions as $x^*_{ij,n}$, $\tau^*_{j,n}$, $W^*_{j,n}$, and $P^*_{n,t}$, and then exit the **for** loop to obtain m_s.
11: **else**
12: **Return** to Step 6 for another iteration in the **for** loop and update $m = m + 1$.
13: **end if**
14: **end for**
15: **end for**
16: **end for**

V. Case Studies

This section evaluates the effectiveness of the online CEV system. Firstly, the setup is shown for simulations. Secondly, the relevant performance metrics and the baseline scenarios for comparison are presented. Thirdly, the proposed model is studied on its effectiveness and effect on the entire system. Fourthly, the proposed model is assessed in different network scales. Lastly, the economic feasibility of the proposed model is examined.

A. Simulation Setup

The performance of the online CEV system is evaluated based on the ride-sharing and V2G coordination operations. the simulations are conducted in the town of Carolina, Alabama[1]. There are totally 56 edges and 26 nodes in this urban region, each with a unique length of road section. 18 meters (59 feet) and 725 meters (2379 feet) are the maximum and minimum edge lengths, respectively. In addition, the system operational time window is selected from 5:00 p.m. to 7:00 p.m. to capture the daily CEV mobility patterns, which can be divided into $|\mathcal{T}| = 120$ slots with $\Delta t = 1$ minutes.

For the settings of the CEV ride-sharing and V2G coordination, the deadline for approaching the final destination is first set equal to the system operational period. For the ride-sharing operation, the number of passengers is set to 10 and the maximum number of CEVs that may be loaded at each edge to 4. Referring to [45], the γ^n and transport costs α_n are set to \$83.68 per hour and \$1.73 per mile, respectively. Furthermore, the final destinations for CEV ride-sharing schemes are randomly selected since they are exactly different from their starting points. On the other hand, for the regulation services, the regulation signal data is exploited on 1 January 2020 [46]. The base regulation reward is set to \$40 per MWh by following [47].

The settings for CEVs are referred to the real-world operations and they are presented in the following. There are two types of CEV groups, e.g. Nissan Leaf with 40 kWh [48] and Chevrolet Volt with 18.4 kWh [49]. The total number of the CEV fleets is $|\mathcal{N}| = 20$. Each CEV is assumed to travel with a fixed velocity of 30 kilometers (18.64 miles) per hour referring to the city average traffic speed. In the meantime, each CEV's unit energy usage β_n is set to 1.112 kWh per kilometers. A single standard coil-set for SAE J2954 charging standard is used for WPT Power Class 1 and 2 up to 7.7kW according to [40]. Then, the discharging and charging power limits are set to -7 kW and 7 kW, respectively. Moreover, the efficiency for charging/discharging is set to 0.9. Besides, the uniform distribution is used to simulate the SOC settings of CEVs, which can be denoted as U[$\cdot$] [28]. Specifically, the CEV n's initial SOC is set to be U[40%, 50%], while the charging fulfillment follows U[0%, 10%]. The charging/discharging mechanism's safety condition is taken into account when the minimum and maximum SOCs are U[10%, 20%] and U[90%, 99%], respectively. Finally, the time-varying unit charging cost λ_n refers to the trend of actual electricity prices in [50].

[1]https://dataverse.harvard.edu/dataset.xhtml?persistentId=doi:10.7910/DVN/CUWWYJ

B. Scenarios for Comparison

Here, the simulations compare four different scenarios so as to evaluate the performance of the proposed online CEV system, which are shown as:

1) S1: Online centralized joint ride-sharing and dynamic V2G scheduling approach in (24)
2) S2: Proposed online bi-level joint approach
3) S3: CEV ride-sharing approach
4) S4: Dynamic V2G scheduling approach [29]

S1 denotes the proposed CEV system with online centralized joint ride-sharing and dynamic V2G scheduling approach, while S2 represents the devised online bi-level CEV algorithm. Meanwhile, for dynamic V2G scheduling, 50% of road segments are assumed to be embedded with PTs in a random manner. For S3, the CEV system is considered unilaterally performing the ride-sharing operation. In this case, this method does not involve the implementation of dynamic V2G scheduling. Besides, for S4, it only considers the provision of V2G service.

S3 is devised based on the centralized ride-sharing approach. In particular, the optimization problem only involves the objective function (15) with the constraints (2) - (4), (6), (7), (19), and (20). Since the optimal operation solutions can be obtained in ride-sharing approach, S3 is set as one benchmark. In S4, each individual CEV's schedule is coordinated by the system via the centralized method [29]. After receiving the regulation signals and the status of CEVs, the system optimizes the subordinate CEVs with their schedules. The results can converge to the global optimum in dynamic V2G scheduling when the forecast information is available and accurate. Hence, S4 can be regarded as another benchmark for assessing the overall performance. All these scenarios are evaluated under the test cases presented in Table II with the detailed analysis shown in the followings.

C. Quality of Ride-sharing Service

The performance of different prediction approaches is evaluated in the quality of ride-sharing services. Here, four metrics are utilized to indicate the overall performance of the provision in the proposed ride-sharing scheme, such as entire system cost, total regulation reward, total ride-sharing cost, and average unit service time. As shown in Table III, both S1 and S2 obtain the relatively high system costs since they provides the joint ride-sharing and charging service. In addition, S2 reaches a bit lower regulation reward in comparison to S4, since S4 only provides CEV dynamic charging services. Considering the ride-sharing cost, since S2 gains a higher value than S3, the time consumed for providing such service in S1 is only marginally higher than S3 for each request. This result also indicates that S2 leads to effective ride-sharing services in the city area. Furthermore, compared to S1, S2 succeeds to achieve near-optimal solutions on overall performance.

D. Effectiveness of V2G regulation service

Then, the performance of different scenarios is evaluated in the provisioning of the V2G regulation service. The standard deviation of the profile is used as the evaluation metric, which is calculated by:

$$\mathrm{Std}(P_{\mathcal{T}}^{\mathrm{tot}}) = \sqrt{\frac{1}{|\mathcal{T}|}\sum_{t\in\mathcal{T}}\left(P_t^{\mathrm{tot}} - \frac{1}{|\mathcal{T}|}(\sum_{t\in\mathcal{T}} P_t^{\mathrm{tot}})\right)^2}. \tag{35}$$

For (35), a better quality of the service is reflected by the smaller value obtained. Since the standard deviation of the original regulation power is $3.79 \times 10^2\ kW$, the effectiveness of the proposed approach is tested for the provisioning of regulation services at various levels of regulation by multiplying the regulation power by 3.5, 7, 8.75, and 10.5 times. The related result is presented in Table IV. The decrease of the standard deviation improves the effectiveness of the proposed system in providing V2G regulation services for S1, S2, and S4. In addition, S2 incurs a better result in the V2G coordination by comparing S4 that only involves dynamic V2G scheduling in the city area. Furthermore, by comparing with S1, S2 can achieve near-optimal solution.

Then, further simulation is done on the effects of various scenarios on grid frequency. Here, the grid frequency standard is set to 50 Hz by following the U.S. standard. Meanwhile, the regulation power is set to the multiplication of 3.5 times. In addition, the operational region shall be the tolerance bound less than 1%, e.g. $[49.5, 50.5]$ Hz, in order to ensure the system stability. Table V indicates that S1, S2, and S4 can all achieve the stability criteria since the three results are close. S3 cannot keep the system stable since it does not provide V2G regulation services. Therefore, it is intuitive that the high quality of the services provided can be guaranteed.

E. Cost/Reward Evaluation under Joint Service

Based on the joint service provided in the town of Carolina, Alabama, the economic benefit associated with various CEV penetration ratios is further analyzed when the system provides the joint service. Here, the performance is evaluated when the regulation power is multiplied by 3.5 times. In real-world operations, each CEV in the system has its own willingness to participate the dynamic wireless charging schemes when providing ride-sharing services. Hence, to assess the economical cost/reward of the joint service, five different cases are considered with 0%, 25%, 50%, 75%, and 100% CEVs in participating the dynamic wireless scheduling schemes, respectively. In Fig. 2, as the number of CEVs in participating both services increases, more system reward is gained and less system operational cost is achieved, which is around 80.81% increase on system reward and 43.71% decrease on system operation cost. In addition, the effectiveness of the devised algorithm on solving the joint problem can be obviously shown with high reward and low system operation cost when the ratio of participated CEVs reaches above 75%.

F. Impact of Different Network Scales and Fleet Sizes

Apart from Carolina city ($N_V = 26, N_E = 56$), the performance in another one large-scale city network is further assessed, namely, Dodge city ($N_V = 66, N_E = 133$). Based on the configurations in Section V-A, the computation time

TABLE II
SIMULATION SCENARIOS FOR COMPARISON.

Test case	Carolina city	Dodge city
Citywise traffic network scale	$(N_V = 26, N_E = 56)$	$(N_V = 66, N_E = 133)$
Percentage of CEV fleet penetration	0%, 25%, 50%, 75%, 100%	0%, 25%, 50%, 75%, 100%
PT placement strategy in S2	no, half, full	no, half, full

TABLE III
COST/REWARD COMPARISON OF DIFFERENT SCENARIOS IN RIDE-SHARING AND V2G SCHEDULING SCHEME.

Scenarios	System cost (US$)	Regulation reward (US$)	Total ride-sharing cost (US$)	Average unit ride-sharing service time (min)
S1	6.53×10^3	6.72×10^2	7.20×10^3	76.30
S2	6.65×10^3	6.70×10^2	7.34×10^3	78.01
S3	4.59×10^3	–	4.59×10^3	71.4
S4	1.01×10^3	1.01×10^3	–	0

TABLE IV
STANDARD DEVIATION OF TOTAL POWER PROFILE IN DIFFERENT REGULATION LEVELS

	Regulation level			
Scenarios	$\sigma = 5.05 \times 10^1\ kW$	$\sigma = 1.01 \times 10^2\ kW$	$\sigma = 1.26 \times 10^2\ kW$	$\sigma = 1.51 \times 10^2\ kW$
S1	$1.68 \times 10^1\ kW$	$5.21 \times 10^1\ kW$	$7.69 \times 10^1\ kW$	$1.02 \times 10^2\ kW$
S2	$1.76 \times 10^1\ kW$	$5.38 \times 10^1\ kW$	$7.72 \times 10^1\ kW$	$1.03 \times 10^2\ kW$
S3	$5.05 \times 10^1\ kW$	$1.01 \times 10^2\ kW$	$1.26 \times 10^2\ kW$	$1.51 \times 10^2\ kW$
S4	$2.50 \times 10^{-3}\ kW$	$1.67 \times 10^1\ kW$	$3.36 \times 10^1\ kW$	$6.08 \times 10^1\ kW$

TABLE V
EFFECT OF CITY SMART GRID FREQUENCY UNDER VARIOUS SCENARIOS

Scenarios	Standard deviation (Hz)	Mean (Hz)
S1	3.08×10^{-1}	50
S2	3.93×10^{-1}	50
S3	1.39×10^1	50
S4	3.07×10^{-1}	50

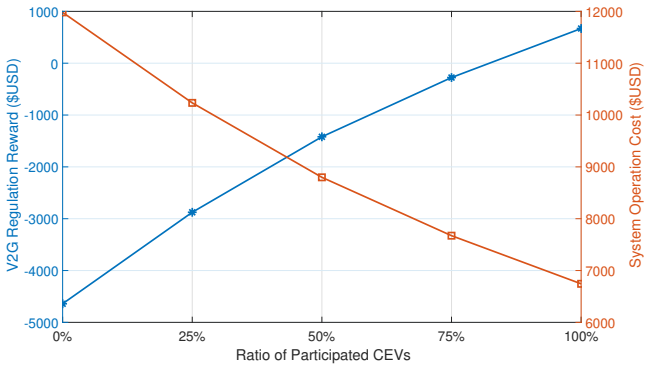

Fig. 2. Cost/Reward evaluation under different ratios of participated CEVs.

is utilized as the evaluation metric for this investigation. In Table VI, it appears that, when traffic network sizes increase, the computation time increases for S1, S2, and S3. In this case, more complicated city traffic networks incur more model constraints. For S4, the computation time does not change significantly since this method does not involve the ride-sharing operations among the city road networks. Besides, S2 achieves a much lower computation time than S1 and S3 because the proposed bi-level joint approach (S2) can greatly reduce the problem complexity in these two cities.

The impact of different fleet size is further studied on the performance of the proposed approaches in Carolina city, which is associated with the scalability of the proposed online approach. In this part, the system performance of four cases is evaluated with 10, 20, 50, and 100 CEVs, respectively. According to the results in Table VII, fleet size expansion raises the system's total ride-sharing cost due to increasing operations involved in more participated CEVs. Besides, the standard deviation of the active power profile in S2 decreases with the increasing number of CEVs, which indicates better performance of the provisioning of the V2G regulation service in the city with more participated CEVs. Furthermore, the mean computation time for S1 increases with more CEVs considered in the traffic networks. The reason is that more CEVs introduce more dimensional variables to the formulated problem, which further increase the computational complexity of the problem. For the mean computation time for S2, it can be reduced greatly, whereas the feasibility and effectiveness of the proposed online model under a large quantity of CEVs

This article has been accepted for publication in IEEE Transactions on Transportation Electrification. This is the author's version which has not been fully edited and content may change prior to final publication. Citation information: DOI 10.1109/TTE.2023.3284423

TABLE VI
COMPUTATION TIMES FOR DIFFERENT NETWORK SCALES WITH 20 CEVS.

$(\mathcal{V}, \mathcal{E})$	(24, 56)	(66, 133)
S1		
Mean computation time (s)	33.60	71.06
S2		
Mean computation time (s)	8.23	59.99
S3		
Mean computation time (s)	112.20	78175.59
S4		
Mean computation time (s)	28.72	29.78

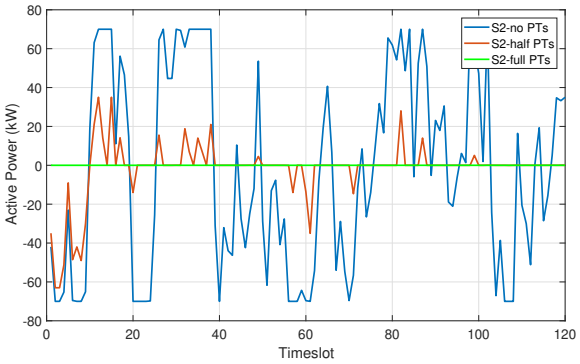

Fig. 3. Effectiveness of V2G Scheduling under different PT placement strategies.

can be demonstrated.

G. Impact of PT placement strategy

The quality of V2G regulation services under different PT placement strategies is evaluated. Here, three different cases are considered in Carolina city, namely, "S2-no PTs", "S2-half PTs", and "S2-full PTs". The first one case presents that it do not involve the PT placement in the traffic networks. Different from this case, "S2-half PTs" denotes that 50% road segments are embedded with PTs, while "S2-full PTs" indicates that all roads are installed over PTs. In particular, for "S2-half PTs", the random strategy is used for the PT placement. Note that the length of each PT is 75 meters. Meanwhile, the regulation power is set to the multiplication of 3.5 times. Through these settings, the performance of the dynamic V2G coordination under different PT placement strategies can be obtained. The result is shown in Fig. 3. Apparently, "S2-full PTs" can achieve the most flatten active power profile while "S2-no PTs" performs the worst. For "S2-half PTs", it can alleviate most fluctuations of the entire profile. However, the insufficient installation of PTs installed over the road segments limits the performance of the dynamic V2G coordination with the provision of V2G regulation services.

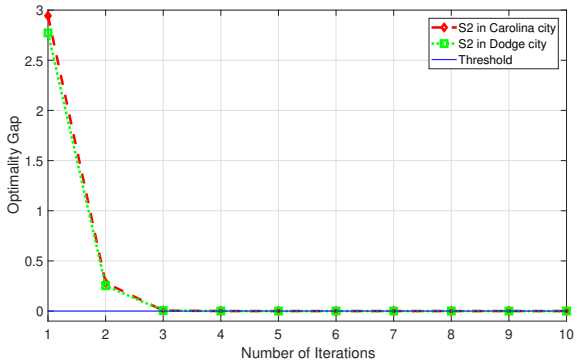

Fig. 4. Iteration process under Benders cuts in different networks.

H. Convergence Analysis

Last but not least, the convergence of the devised online bi-level algorithm is assessed, known as Algorithm 1. The threshold gap of this algorithm is calculated in (34), which is related to the optimal solutions obtained by S1 and S2. In this part, the threshold gap is set to 10^{-4}. As shown in Fig. 4, it can be observed that both curves successfully achieve optimal values convergence after a certain number of iterations. Specifically, the case "S2 in Carolina city" reaches the threshold around 3 iterations while the case "S2 in Dodge city" reaches the equilibrium after around 4 rounds. As a result, the devised online bi-level algorithm reaches the optimal values much quicker. Also, the converged optimal objective values of this algorithm in these two cities are not equivalent due to the complexity of the problem that is related to scale of the road networks.

VI. CONCLUSIONS

This paper proposes an online CEV system for joint ride-sharing and dynamic V2G coordination in smart cities. To implement the combined operations, the joint problem is formulated. In order to deal with the forecast uncertainties, this paper thereby formulates an online scheduling problem, as well as devising an online distributed algorithm. Meanwhile, the communication effect is tackled between the interactions of CEVs and the control center. The case studies show that the proposed model guarantees the effectiveness of both the citywise ride-sharing and V2G regulation services via the reliable vehicular communications. Additionally, the computational time of the proposed online bi-level algorithm can be greatly reduced with different network scales. Furthermore, with the increasing number of CEV fleets, the entire system operation cost can be significantly reduced around 43.71%, in which the system reward can be increased by 80.81%. Meanwhile, the grid stability issue can indeed be alleviated. In the future, wired charging possibilities will be incorporated along with the existing wireless ones for CEVs in a city area. In addition, an incentive mechanism can be applied to motivate CEVs to participate the system.

TABLE VII
IMPACT OF DIFFERENT FLEET SIZE OF CEVS IN CAROLINA CITY.

Number of CEVs	10	20	50	100
Total ride-sharing cost (S1) (US$)	3.09×10^2	7.20×10^3	1.89×10^4	3.47×10^4
Total ride-sharing cost (S2) (US$)	3.32×10^2	7.34×10^3	1.66×10^4	3.14×10^4
Standard deviation of active power profile (S1) (kW)	7.37×10^1	1.68×10^1	1.47×10^1	1.31×10^1
Standard deviation of active power profile (S2) (kW)	2.52×10^1	1.76×10^1	2.73×10^0	1.45×10^0
Mean Computation time (S1) (min)	17.60	33.60	81.60	161.60
Mean Computation time (S2) (min)	6.82	8.23	10.42	15.06

REFERENCES

[1] N. Lu, N. Cheng, N. Zhang, X. Shen, and J. W. Mark, "Connected vehicles: Solutions and challenges," *IEEE Internet of Things Journal*, vol. 1, no. 4, pp. 289–299, Aug. 2014.

[2] S. Chen, J. Hu, Y. Shi, Y. Peng, J. Fang, R. Zhao, and L. Zhao, "Vehicle-to-everything (v2x) services supported by lte-based systems and 5g," *IEEE Communications Standards Magazine*, vol. 1, no. 2, pp. 70–76, 2017.

[3] Z. Niu, X. S. Shen, Q. Zhang, and Y. Tang, "Space-air-ground integrated vehicular network for connected and automated vehicles: Challenges and solutions," *Intelligent and Converged Networks*, vol. 1, no. 2, pp. 142–169, Sep. 2020.

[4] Z. Qu, J. Wang, and R. A. Hull, "Cooperative control of dynamical systems with application to autonomous vehicles," *IEEE Transactions on Automatic Control*, vol. 53, no. 4, pp. 894–911, May 2008.

[5] A. B. T. Sherif, K. Rabieh, M. M. E. A. Mahmoud, and X. Liang, "Privacy-preserving ride sharing scheme for autonomous vehicles in big data era," *IEEE Internet of Things Journal*, vol. 4, no. 2, pp. 611–618, Apr. 2017.

[6] B. Cao, L. Alarabi, M. F. Mokbel, and A. Basalamah, "Sharek: A scalable dynamic ride sharing system," in *2015 16th IEEE International Conference on Mobile Data Management*, vol. 1, Jun. 2015, pp. 4–13.

[7] Y. Luo, X. Jia, S. Fu, and M. Xu, "pride: Privacy-preserving ride matching over road networks for online ride-hailing service," *IEEE Transactions on Information Forensics and Security*, vol. 14, no. 7, pp. 1791–1802, Jul. 2019.

[8] S. Ma, Y. Zheng, and O. Wolfson, "Real-time city-scale taxi ridesharing," *IEEE Transactions on Knowledge and Data Engineering*, vol. 27, no. 7, pp. 1782–1795, Jul. 2015.

[9] R. Engelhardt, F. Dandl, A. Bilali, and K. Bogenberger, "Quantifying the benefits of autonomous on-demand ride-pooling: A simulation study for munich, germany," in *2019 IEEE Intelligent Transportation Systems Conference (ITSC)*, Oct. 2019, pp. 2992–2997.

[10] F. Dandl and K. Bogenberger, "Comparing future autonomous electric taxis with an existing free-floating carsharing system," *IEEE Transactions on Intelligent Transportation Systems*, vol. 20, no. 6, pp. 2037–2047, Jun. 2019.

[11] G. Guo and Y. Xu, "A deep reinforcement learning approach to ride-sharing vehicles dispatching in autonomous mobility-on-demand systems," *IEEE Intelligent Transportation Systems Magazine*, 2020.

[12] A. Y. S. Lam, Y. Leung, and X. Chu, "Autonomous-vehicle public transportation system: Scheduling and admission control," *IEEE Transactions on Intelligent Transportation Systems*, vol. 17, no. 5, pp. 1210–1226, May 2016.

[13] M. Zhu, X. Liu, and X. Wang, "An online ride-sharing path-planning strategy for public vehicle systems," *IEEE Transactions on Intelligent Transportation Systems*, vol. 20, no. 2, pp. 616–627, Feb. 2019.

[14] W. Zeng, Y. Han, W. Sun, and S. Xie, "Exploring the ridesharing efficiency of taxi services," *IEEE Access*, vol. 8, pp. 160 396–160 406, Sep. 2020.

[15] I. Hwang, Y. J. Jang, Y. D. Ko, and M. S. Lee, "System optimization for dynamic wireless charging electric vehicles operating in a multiple-route environment," *IEEE Transactions on Intelligent Transportation Systems*, vol. 19, no. 6, pp. 1709–1726, Jun. 2018.

[16] A. Y. Lam, K.-C. Leung, and V. O. Li, "Vehicular energy network," *IEEE Transactions on Transportation Electrification*, vol. 3, no. 2, pp. 392–404, Jun. 2017.

[17] A. Y. S. Lam and V. O. K. Li, "Opportunistic routing for vehicular energy network," *IEEE Internet of Things Journal*, vol. 5, no. 2, pp. 533–545, Apr. 2018.

[18] A. Zaheer, M. Neath, H. Z. Z. Beh, and G. A. Covic, "A dynamic ev charging system for slow moving traffic applications," *IEEE Transactions on Transportation Electrification*, vol. 3, no. 2, pp. 354–369, Jun. 2017.

[19] D. Kosmanos, L. A. Maglaras, M. Mavrovouniotis, S. Moschoyiannis, A. Argyriou, A. Maglaras, and H. Janicke, "Route optimization of electric vehicles based on dynamic wireless charging," *IEEE Access*, vol. 6, pp. 42 551–42 565, Jul. 2018.

[20] H. Zhang, F. Lu, and C. Mi, "An electric roadway system leveraging dynamic capacitive wireless charging: Furthering the continuous charging of electric vehicles," *IEEE Electrification Magazine*, vol. 8, no. 2, pp. 52–60, Jun. 2020.

[21] X. Tang, C. Sun, S. Bi, S. Wang, and Y.-J. A. Zhang, "A holistic review on advanced bi-directional ev charging control algorithms," *ACM SIGEnergy Energy Informatics Review*, Nov. 2021.

[22] C. Liu, K. T. Chau, D. Wu, and S. Gao, "Opportunities and challenges of vehicle-to-home, vehicle-to-vehicle, and vehicle-to-grid technologies," *Proceedings of the IEEE*, vol. 101, no. 11, pp. 2409–2427, Nov. 2013.

[23] A. Ahmad, M. S. Alam, and R. Chabaan, "A comprehensive review of wireless charging technologies for electric vehicles," *IEEE Transactions on Transportation Electrification*, vol. 4, no. 1, pp. 38–63, Mar. 2018.

[24] K. Tachikawa, M. Kesler, and O. Atasoy, "Feasibility study of bi-directional wireless charging for vehicle-to-grid," *SAE Technical Paper 2018-01-0669*, Apr. 2018.

[25] A. Y. S. Lam, J. J. Q. Yu, Y. Hou, and V. O. K. Li, "Coordinated autonomous vehicle parking for vehicle-to-grid services: Formulation and distributed algorithm," *IEEE Transactions on Smart Grid*, vol. 9, no. 5, pp. 4356–4366, Sep. 2018.

[26] W. Kempton and J. Tomić, "Vehicle-to-grid power fundamentals: Calculating capacity and net revenue," *Journal of Power Sources*, vol. 144, no. 1, pp. 268 – 279, 2005.

[27] ——, "Vehicle-to-grid power implementation: From stabilizing the grid to supporting large-scale renewable energy," *Journal of Power Sources*, vol. 144, pp. 280–294, Jun. 2005.

[28] S. Zhang and K.-C. Leung, "Joint optimal power flow routing and vehicle-to-grid scheduling: Theory and algorithms," *IEEE Transactions on Intelligent Transportation Systems*, vol. 23, no. 1, pp. 499–512, Jan. 2022.

[29] S. Zhang and J. J. Q. Yu, "Electric vehicle dynamic wireless charging system: Optimal placement and vehicle-to-grid scheduling," *IEEE Internet of Things Journal*, vol. 9, no. 8, pp. 6047–6057, Apr. 2022.

[30] T. Litman, "Introduction to multi-modal transportation planning," *Victoria Transport Policy Institute*, Jan. 2011.

[31] K.-F. Chu, A. Y. S. Lam, and V. O. K. Li, "Joint rebalancing and vehicle-to-grid coordination for autonomous vehicle public transportation system," *IEEE Transactions on Intelligent Transportation Systems*, 2021.

[32] S. Zhang and K.-C. Leung, "A smart cross-system framework for joint allocation and scheduling with vehicle-to-grid regulation service," *IEEE Transactions on Vehicular Technology*, vol. 71, no. 6, pp. 6019–6031, Jun. 2022.

[33] J. J. Q. Yu and A. Y. S. Lam, "Autonomous vehicle logistic system: Joint routing and charging strategy," *IEEE Transactions on Intelligent Transportation Systems*, vol. 19, no. 7, pp. 2175–2187, Jul. 2018.

[34] X. Tang, S. Bi, and Y.-J. A. Zhang, "Distributed routing and charging scheduling optimization for internet of electric vehicles," *IEEE Internet of Things Journal*, vol. 6, no. 1, pp. 136–148, Feb. 2019.

[35] J. Shi, Y. Gao, W. Wang, N. Yu, and P. A. Ioannou, "Operating electric vehicle fleet for ride-hailing services with reinforcement learning," *IEEE Transactions on Intelligent Transportation Systems*, vol. 21, no. 11, pp. 4822–4834, Nov. 2020.

[36] M. B. Mollah, J. Zhao, D. Niyato, Y. L. Guan, C. Yuen, S. Sun, K.-Y. Lam, and L. H. Koh, "Blockchain for the internet of vehicles towards intelligent transportation systems: A survey," *IEEE Internet of Things Journal*, vol. 8, no. 6, pp. 4157–4185, Mar. 2021.
[37] B. Fan, Y. Wu, Z. He, Y. Chen, T. Q. Quek, and C.-Z. Xu, "Digital twin empowered mobile edge computing for intelligent vehicular lane-changing," *IEEE Network*, vol. 35, no. 6, pp. 194–201, Nov./Dec. 2021.
[38] B. Zhou, K. Zhang, K. W. Chan, C. Li, X. Lu, S. Bu, and X. Gao, "Optimal coordination of electric vehicles for virtual power plants with dynamic communication spectrum allocation," *IEEE Transactions on Industrial Informatics*, vol. 17, no. 1, pp. 450–462, Jan. 2021.
[39] J. Dai and D. C. Ludois, "A survey of wireless power transfer and a critical comparison of inductive and capacitive coupling for small gap applications," *IEEE Transactions on Power Electronics*, vol. 30, no. 11, pp. 6017–6029, Nov. 2015.
[40] *Wireless Power Transfer for Light-Duty Plug-In/Electric Vehicles and Alignment Methodology*, SAE Standard J2954, Nov. 2017.
[41] J. Shin, S. Shin, Y. Kim, S. Ahn, S. Lee, G. Jung, S.-J. Jeon, and D.-H. Cho, "Design and implementation of shaped magnetic-resonance-based wireless power transfer system for roadway-powered moving electric vehicles," *IEEE Transactions on Industrial Electronics*, vol. 61, no. 3, pp. 1179–1192, Mar. 2014.
[42] Q. Dong, D. Niyato, and P. Wang, "Dynamic spectrum access for meter data transmission in smart grid: Analysis of packet loss," in *2012 IEEE Wireless Communications and Networking Conference (WCNC)*, Apr. 2012.
[43] C. Yang, J. Yao, W. Lou, and S. Xie, "On demand response management performance optimization for microgrids under imperfect communication constraints," *IEEE Internet of Things Journal*, vol. 4, no. 4, pp. 881–893, Aug. 2017.
[44] R. Rahmaniani, T. G. Crainic, M. Gendreau, and W. Rei, "The Benders decomposition algorithm: A literature review," *European Journal of Operational Research*, vol. 259, no. 3, pp. 801–817, 2017.
[45] A. Izadi, M. Nabipour, and O. Titidezh, "Cost models and cost factors of road freight transportation: A literature review and model structure," *Fuzzy Information and Engineering*, pp. 1–21, Jan. 2020.
[46] "RTO Regulation Signal Data," PJM, Jan. 2020. [Online]. Available: https://www.pjm.com/markets-and-operations/ancillary-services.aspx.
[47] "PJM Regulation Zone Preliminary Billing Data," PJM, Oct. 2020. [Online]. Available: https://dataminer2.pjm.com/feed/reg_zone_prelim_bill/definition.
[48] Nissan. (2014, May). *Leaf Specifications* [Online]. Available: http://www.nissanusa.com/electric-cars/leaf/versions-specs/.
[49] Chevrolet. (2018, March). *Volt Specifications* [Online]. Available: http://www.chevrolet.com/electric/volt-plug-in-hybrid.
[50] "Day-ahead prices," Nord Pool, Dec. 2021. [Online]. Available: https://www.nordpoolgroup.com/en/Market-data1/Dayahead/Area-Prices/de-lu/hourly/?view=table.

Shiyao Zhang (S'18–M'20) received the B.S. degree (Hons.) in Electrical and Computer Engineering from Purdue University, West Lafayette, IN, USA, in 2014, the M. S. degree in Electrical Engineering (Electric Power) from University of Southern California, Los Angeles, CA, USA, in 2016, and the Ph.D. degree from the University of Hong Kong, Hong Kong, China. He was a Post-Doctoral Research Fellow with the Academy for Advanced Interdisciplinary Studies, Southern University of Science and Technology from 2020 to 2022. He is currently a Research Assistant Professor with the Research Institute for Trustworthy Autonomous Systems, Southern University of Science and Technology. His research interests include smart cities, intelligent transportation systems, smart energy systems, optimization theory and algorithms, and deep learning applications.

James J. Q. Yu (S'11–M'15–SM'20) is an assistant professor at the Department of Computer Science and Engineering, Southern University of Science and Technology, Shenzhen, China, and an honorary assistant professor at the Department of Electrical and Electronic Engineering, the University of Hong Kong. He received the B.Eng. and Ph.D. degree in electrical and electronic engineering from the University of Hong Kong, Pokfulam, Hong Kong, in 2011 and 2015, respectively. He was a post-doctoral fellow at the University of Hong Kong from 2015 to 2018. His general research interests are in smart city and privacy computing, deep learning, intelligent transportation systems, and smart energy systems. His work is now mainly on forecasting and decision making of future transportation systems and artificial intelligence techniques for industrial applications. He was listed in the World's Top 2% Scientists of from 2020 to 2022 by Stanford University, ranked at top 0.32% of all Artificial Intelligence scholars. He is an Editor of the IET SMART CITIES journal and a Senior Member of IEEE.